KonTur-Results (continued from issue 1/85 pages 1 to 52 and issue 2/85 pages 237 to 272)

Rotating Clouds Within Cloud Streets

Thomas Hauf

Institut für Physik der Atmosphäre, DFVLR Oberpfaffenhofen

(Manuscript received 10.07.1984, in revised form 29.04.1985)

Abstract:

In a case study a maritime cloud street system is investigated. Aircraft measurements show that most of the clouds were found to be embedded in a vortex with vertical axis of rotation. The vortex diameter varied between 500 m – 2300 m and was comparable to the cloud diameter. Maximum rotation velocity was about 2 m/s. No preferred sign of rotation was found. The rotation is explained with the advection process and the vorticity production caused by the convergence in the lower half of the roll circulation system. Based on the helicity concept some implications of cloud rotation are discussed and some conclusions are drawn regarding scale interaction processes.

Zusammenfassung: Rotierende Wolken in Wolkenstraßen

In einer Fallstudie wird ein maritimes Wolkenstraßensystem untersucht. Flugzeugmessungen zeigen, daß die meisten der untersuchten Wolken in Wirbel eingebettet sind und sich mit diesen um eine vertikale Achse drehen. Der Wirbeldurchmesser liegt zwischen 500 m und 2300 m und ist ungefähr gleich dem Wolkendurchmesser. Die größten Rotationsgeschwindigkeiten im Wirbel betragen annähernd 2 m/s. Ein bevorzugter Drehsinn wurde nicht gefunden. Die Rotation der Wolken kann mit Advektion und Vorticityproduktion als Folge der Konvergenz in der unteren Hälfte der Rollenzirkulation erklärt werden. Unter Verwendung des Helizitätsbegriffes werden einige Schlußfolgerungen aus der Wolkenrotation gezogen und speziell im Hinblick auf Skalenwechselwirkungsprozesse diskutiert.

Résumé: Nuages en rotations au sein de rues de nuages

Il s'agit de l'étude d'un cas particulier d'un système de rues de nuages maritimes. Des mesures aéroportées montrent que la plupart des nuages étudiés est enveloppée par des rouleaux aux axes de rotation verticaux. Le diamètre du rouleau varie entre 500 m et 2300 m, il est comparable au diamètre des nuages. La vitesse maximale de rotation est de 2 m/s environ. On n'a pas trouvé de sens de rotation préféré. La rotation s'explique par l'advection et la production de vorticity résultant de convergence dans la moitié inférieure de la circulation en rouleaux. La conception d'hélicité permet certaines conclusions sur la rotation des nuages qui sont discutées surtout sous l'aspect de l'interaction d'échelles.

1 Introduction

The organization of convective clouds in parallel lines is a very common feature of atmospheric boundary layer flow. Lines or streets of clouds can be clearly identified on satellite pictures. Cloud streets indicate longitudinal rolls which form as a secondary flow in the PBL. The roll axis is horizontal and nearly parallel to the mean wind.

0005-8173/85/03 0380–19 $ 03.00/0

Cloud streets have been observed for decades and the collected observational material now gives a clear insight into the structure of the roll circulation and the conditions under which cloud streets are formed (KUETTNER, 1959, 1971; LeMONE, 1973; LeMONE and PENNELL, 1976; MÜLLER, 1984; BRÜMMER, 1985).

Theoretical studies based on perturbation techniques and on numerical simulations can explain certain features of roll circulation, although the assumptions underlying these investigations differ substantially (BROWN, 1974, 1980). Roll structure may result either from pure convective instability or from pure dynamical instability or from a combination of both.

In most cases cloud streets are composed of individual clouds aligned in rows (Figure 1). Therefore, cloud streets often are described as "strings of pearls".

Cloud bands as one might expect from two-dimensional theoretical and numerical investigations are observed only occasionally. One of such a case is described by WALTER and OVERLAND (1984).

The existence of individual clouds indicates that besides the mean flow and the roll circulation at least one further scale is present.

Most emphasis of theory and observation, however, is laid on the roll circulation while motions on the smaller cloud scale are investigated by only a few authors.

In this paper one special feature of single clouds within cloud streets is investigated. It is our objective to present experimental data which show that clouds within cloud streets rotate vertically.

The cloud rotation is seen as a result of scale interaction mechanisms between the roll scale, the cloud scale and the turbulent scale. Two processes are considered: advection and vorticity production. The importance of both processes for motions in scale smaller than the roll scale results from the significant dynamical structure of the roll circulation.

The *advection* process and its impact on smaller scale motion was treated extensively by LeMONE and PENNELL (1976), in the following referred to as LMP. They found that in cloud streets under suppressed

• **Figure 1**
Cloud streets over the North Sea. Observed during the KonTur experiment on 29.9.1981 at a height of 3500 m.

conditions water vapor, vertical velocity and turbulence are concentrated in the central upwelling region. The concentration is caused by turbulent eddies which are collected by horizontal convergence in the lower layer and transported upwards by the upward vertical velocity. Clouds are formed when the turbulent and moist air parcels reach the lifting condensation level. LMP suggested that the "strings of pearls" are just a simple organization of convective and turbulent elements into rows by roll circulation. The increase of turbulent kinetic energy in the upwelling region as well as the arrangement of clouds in lines are seen as by-products of the roll system. No interaction, however, is assumed to exist between the various scales involved. Budget considerations of turbulent kinetic energy based on observations by LeMONE (1973, 1976), in the following referred to as LM1 and LM2, confirm these findings. The authors concluded that roll circulation affects the subscale motion by advection only.

Besides advection, however, a second important interaction process has to be considered, which is the *vorticity production* due to the convergence in the lower part of the roll circulation.

It is the general hypothesis of this paper that by advection and vorticity production a sufficient explanation of cloud rotation can be given.

Two cases are considered differing substantially in their assumptions. In the first the impact of roll circulation on turbulent motions is investigated. It is assumed that the scaling of clouds and the existence of individual clouds is determined or at least essentially influenced by the advection and vorticity production processes. In the second case we assume the cloud scale with individual clouds to be given and investigate the impact of roll circulation on them. In both cases cloud rotation can be explained.

The cloud rotation is discussed in the light of the helicity concept. A nonzero helicity $H = \mathbf{v} \cdot (\nabla \times \mathbf{v})$ is one of the important consequences of cloud rotation. Helical flow structures are known to be less dissipative compared to nonhelical ones. Their lifetimes, therefore, are increased and due to this they can contribute to an inverse energy cascade (LEVICH and TZVETKOV, 1984) feeding energy to larger scale flow structures. This argument offers an interesting feed back mechanism between the roll scale and the cloud scale.

In the next section some theoretical arguments concerning vorticity and helicity are presented, whereas the experimental proof of cloud rotation follows in the adjacent sections.

2 Theory

2.1 The vorticity budget

The most striking feature of the roll circulation is convergence in lower and divergence in upper levels, as schematically depicted in Figure 2. The advection due to this confluence and diffluence leads to a collecting effect in the lower part and to a distributing effect in the upper part. This was discussed previously by other authors and we refer to LMP, LM1, and LM2 for further details. The advection mechanism for the given flow structure is quite obvious and needs no further explanation. We, therefore, focus our interest on another feature of a convergent or divergent wind field and we look at those dynamical quantities for which horizontal divergence or convergence acts as a source or a sink. This immediately leads to the vorticity. Its budget equation can be derived from the momentum equation

$$\frac{D}{Dt}(\rho \mathbf{v}) + \nabla p = -\rho g \mathbf{k} \tag{1}$$

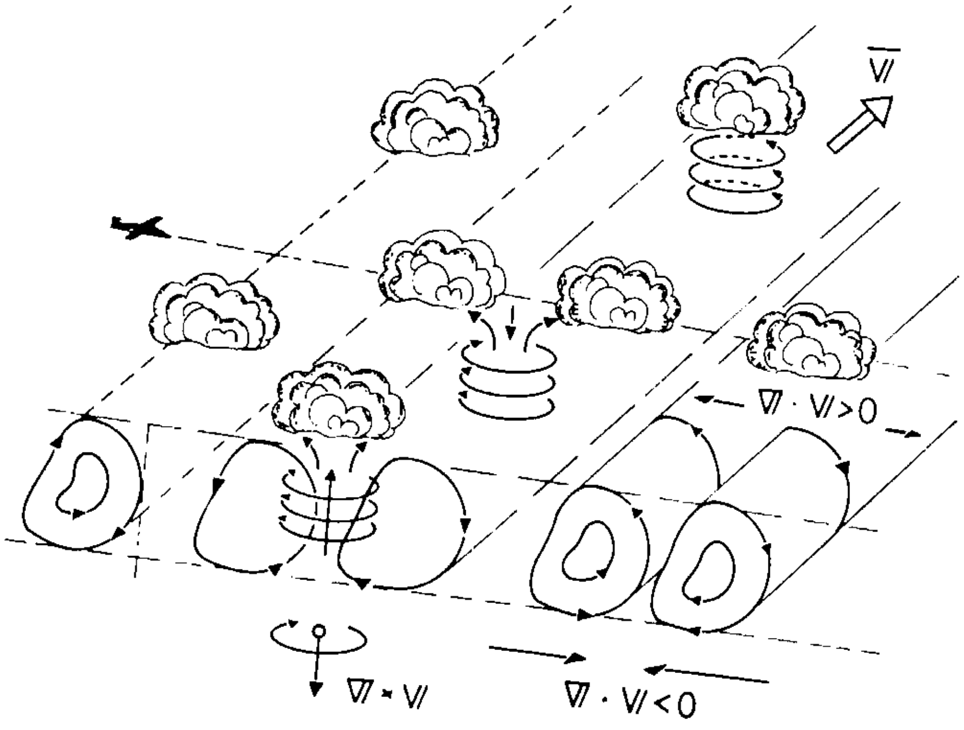

• **Figure 2**
Schematic illustration of cloud street circulation with embedded vortices. The vortex in the middle of the figure refers to the case study described in section 4.5. The cloud consists of two bodies with weak subsidence in between.

ignoring Coriolis force and viscous forces:

$$\frac{D}{Dt}\rho(\nabla \times \mathbf{v}) + \rho(\nabla \times \mathbf{v})(\nabla\cdot\mathbf{v}) - \underbrace{\rho(\nabla \times \mathbf{v})\cdot\nabla\mathbf{v}}_{\text{shear}} - \underbrace{\frac{1}{\rho}\nabla\rho \times \nabla p}_{\text{baroclinicity}} = 0 \tag{2}$$

where

$$\frac{D}{Dt}\rho\phi = \frac{\partial\rho\phi}{\partial t} + \nabla\cdot\mathbf{v}\rho\phi \tag{3}$$

is the budget operator.

Under these assumptions the well-known shear production term and the baroclinicity production term are found. Regarding the vertical vorticity component $\zeta = \mathbf{k}\cdot(\nabla \times \mathbf{v})$, the budget equation can be written as follows:

$$\begin{aligned}\frac{D}{Dt}\rho\zeta &= -\rho\zeta(\nabla_h\cdot\mathbf{v}_h) - \rho(\nabla_h w \times \partial_z\mathbf{v}_h) + \frac{1}{\rho}\mathbf{k}\cdot(\nabla\rho \times \nabla p) = \\ &= \underbrace{-\rho\zeta(\partial_x u + \partial_y v)}_{\text{divergence term}} - \underbrace{\rho(\partial_x w\,\partial_z v - \partial_y w\,\partial_z u)}_{\text{twisting term}} + \underbrace{\frac{1}{\rho}\mathbf{k}\cdot(\nabla\rho \times \nabla p)}_{\text{baroclinicity term}}\end{aligned} \tag{4}$$

with ∇_h, $\mathbf{v}_h$ horizontal vectors and using Cartesian coordinates. Equation (4) shows that vorticity can be changed locally by four processes:

1. *Advection.* It is represented by $\nabla\cdot w\rho\zeta$ in the budget operator (cf. Equation (3)).
2. *Divergence* or convergence of the horizontal wind field.
3. *Twisting* of horizontal vortices into the vertical.
4. *Baroclinicity* with nonparallel isobaric and isochoric or isothermic surfaces.

In the following we consider the advection process and the divergence term $-\rho\zeta\nabla_h \cdot v_h$ as the only vorticity source term. The vorticity production by twisting as well as by baroclinicity is not investigated. This, however, does not mean that both terms in general are small compared with the divergence term. If, for instance, the development of the roll circulation itself is considered, then twisting and baroclinicity are important factors and cannot be ignored.

It, therefore, might happen that not only advection and divergence are important processes for the development and behaviour of clouds within cloud streets but also and possibly to a much greater extent twisting and baroclinicity. The attempted explanation of cloud rotation, therefore, might be incomplete and might miss important physical processes. The author is aware of this fact.

Conclusive answers to these questions can be given by 3-D numerical simulations only.

The vorticity equation is therefore considered in a reduced form only:

$$\frac{D}{Dt}\rho\zeta = -\rho\zeta\,\nabla_h \cdot v_h \tag{5}$$

As we are interested in the impacts of roll motion on small scale motions, v_h in the divergence term in the following is understood as the roll scale motion and is assumed to be given. ζ denotes the vorticity of the cloud scale and/or the turbulent scale.

Equation (5) means that in a convergent wind field like the roll circulation system with $\nabla_h \cdot v_h < 0$ vorticity is enhanced. It should be noted that the source strength of vorticity production is dependent on the vorticity itself. This implies that amplification of vorticity is only possible if the vorticity is unequal zero. The roll convergence mechanism, therefore, to be effective needs a vorticity producing process on scales smaller than the roll scale. The vorticity provided by this process could then be amplified by the roll convergence mechanism.

Now we consider two different cases. First we look at the vorticity on the turbulent scale which is associated with thermals or turbulent eddies. Secondly, we discuss the vorticity on the cloud scale associated with individual clouds.

Case (i) *ζ turbulent vorticity*

Turbulence is produced either by shear or by buoyancy. Roll circulation is a typical boundary layer phenomenon and in many cases driven by the mean wind shear, as in the one case discussed lateron in this paper. The mean wind shear generates eddies especially in the lower levels of the roll system. Under convective situations turbulence is also created by rising thermals. Both processes contribute to cloud scale fluctuations of the flow field. With each eddy or thermal a certain amount of vorticity is associated. These flow structures are embedded in the convergent wind field of the roll circulation. Thus they are advected and concentrated in the central updraft core where as a result turbulent kinetic energy reaches its maximum (BROWN, 1974; LMP).

As the vorticity field of each eddy or thermal is enhanced by convergence, the cloud source region is also a region of strong vorticity amplification.

In contrast to advection, which only transports vorticity to the central core, convergence is a real source of vorticity. Both effects are described by Equation (5).

Following BROWN's (1980) calculations the divergence term in the vorticity budget is estimated as

$$D = \nabla_h \cdot v_h \sim -3\ \mathrm{m/s}/3\ \mathrm{km} = -10^{-3}\ \mathrm{s}^{-1}.$$

This means that the vorticity of each eddy or thermal is amplified:

$$\zeta(t) = \zeta_0\, e^{-Dt}$$

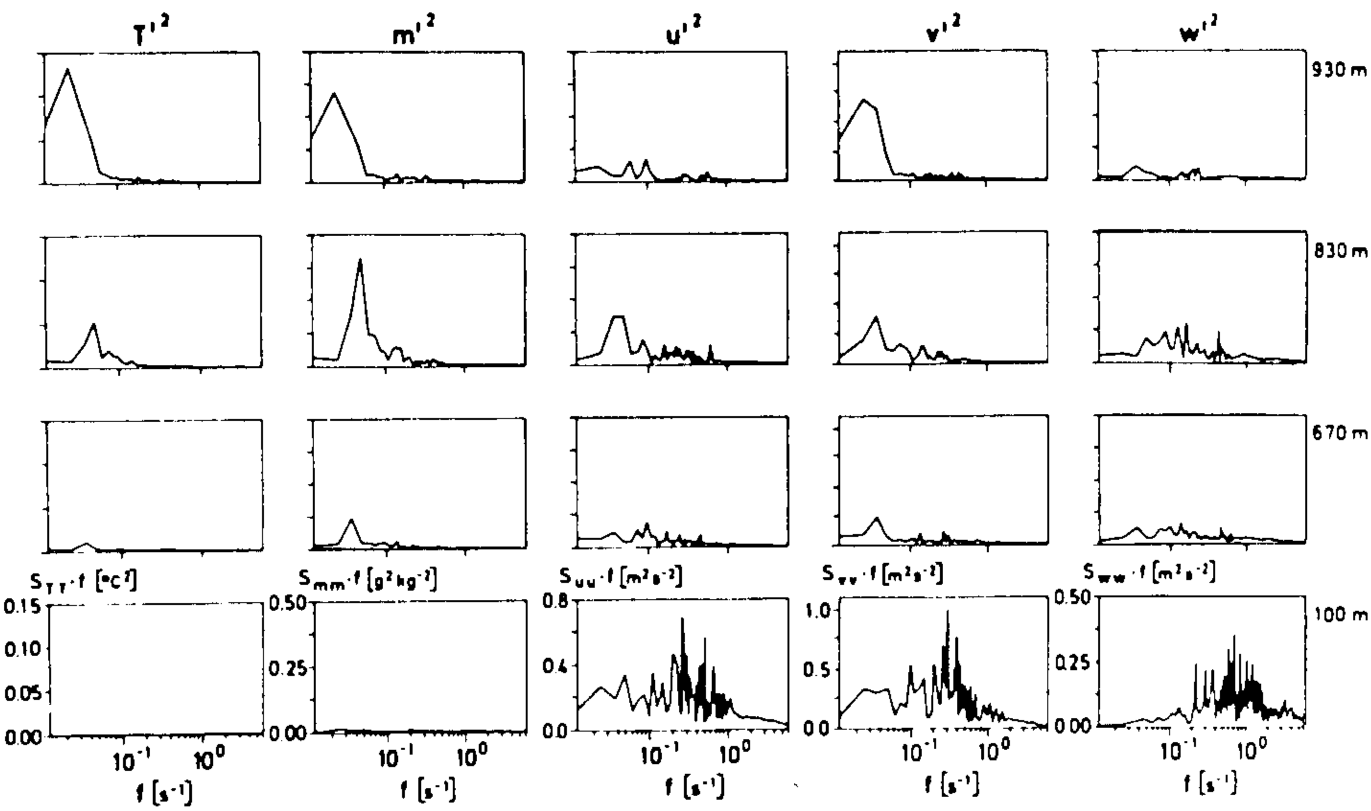

• **Figure 3** Variance spectra of temperature (T), mixing ratio (m), E-W (u), N-S (v) and vertical (w) wind component for flight legs at four levels perpendicular to cloud streets. After BRÜMMER et al. (1982) (with courtesy of the authors).

with a time constant of 16 min, which is also equivalent to the travelling time between the subsidence region and the upwelling region.

During the transport to the cloud source region and along the updraft the airparcels start to rotate. Their rotation expressed by the vorticity is increased. It is suggestive to assume that they also increase in size, possibly due to merging. The increase in size is in agreement with the observed increase in length scale with height as documented by measured power spectra (cf. Figure 3).

The combined effect of advection, vorticity amplification and growing of thermals results in turbulent and buoyant vortices, which are centred in the convergence region. The updraft stretches the vortices and increases their vertical extension. Thus some of them might temporarily extend down to such low heights where the updraft of the roll circulation nearly vanishes. As a consequence of this hypothesis strong horizontal wind fluctuations on the cloud scale should be found in low heights.

The vorticity of the vortices centred in the updraft core is continuously amplified until equilibrium between production and dissipation of vorticity is reached. Dissipation of vorticity, however, is not described by Equation (5).

If the lifting condensation level is reached clouds are formed. They are embedded in the vortices and rotate with them. Cloud rotation, therefore, is caused by vortices centred in the upwelling region. The vortices themselves are a result of low level advection and vorticity production.

The physical picture just developed suggests that the merging of thermals and their increase in size lead finally to individual clouds. In this picture low level advection and vorticity production essentially influence or even determine this scaling process. It, however, should be noted that the physical mechanisms which are responsible for the existence of single clouds and thus for the cloud scale are presently not fully understood. It will be the subject of future investigations to give a conclusive answer to those questions. Numerical simulations, especially of cloud streets under convective and shear conditions, are needed to clarify the cloud scaling mechanism and the importance of advection and vorticity production for this mechanism.

Case (ii): *ζ vorticity on the cloud scale*

We now consider the vorticity on the cloud scale, which is associated with individual clouds or convective plumes. Thus we assume the cloud scale to be given with individual clouds selected by a nonlinear mechanism not investigated here. The advection process arranges the clouds in lines along the updraft region, as already suggested by LMP. It also transports moisture and heat in the lower levels to the cloud source region thus feeding the clouds. The divergence effect amplifies the vorticity of each individual cloud till an equilibrium is reached between production and dissipation of vorticity similar to the previous case. Due to the permanent vorticity enhancement clouds finally rotate. They are congruent with or at least embedded in vortices centred in the updraft core.

Both cases agree in that cloud rotation is sufficiently explained by advection and vorticity production in the lower levels of the roll circulation. They differ in to what degree both processes influence or even determine the scaling of clouds. To answer the latter problem is beyond the scope of this paper as stated previously.

The developed picture can be illustrated by looking at a bath tub vortex where the hole in the bath is replaced by a slot. By analogy to the bath tub vortex, it is assumed that the rotation axis of the sub-roll scale vortices, which are captured in the central updraft core is mainly vertical. In contrast to roll circulation, however, vorticity of the bath tub vortex is generated at the wall and is not of turbulent or convective origin.

The sense of rotation should be equally distributed as there is no preferred sign of turbulent vorticity in the atmospheric boundary layer. Because of their turbulent origin it is expected that, unlike in von Karman's vortex streets, vortices in the central updraft core are unordered. Thus the spacing should be greater because of opposing radial velocities. In the upper level of roll circulation divergence will damp the rotation and limit the vortices in their vertical extension.

2.2 Helicity

In some recent papers the importance of helicity for the development and persistence of atmospheric flow structures is suggested (LILLY, 1984; ETLING, 1985; LEVICH and TZVETKOV, 1984). Helicity is defined as the inner product between velocity and rotation: $H = \mathbf{v} \cdot (\nabla \times \mathbf{v})$.

If clouds within cloud streets rotate then their helicity is unequal zero, because the updraft is parallel to the rotation vector. This holds also for any rotating updraft. In the following we will look at this special aspect of cloud rotation. For illustration we write the momentum equation in the form:

$$\frac{\partial \mathbf{v}}{\partial t} + \frac{\nabla \mathbf{v} \times \mathbf{v}}{2} + (\nabla \times \mathbf{v}) \times \mathbf{v} = -\frac{1}{\rho} \nabla p - g\mathbf{k} \tag{6}$$

and also the rotation budget:

$$\frac{\partial (\nabla \times \mathbf{v})}{\partial t} + \nabla \times [(\nabla \times \mathbf{v}) \times \mathbf{v}] - \frac{1}{\rho} \nabla \rho \times \nabla p = 0 \tag{7}$$

Helicity is maximum if the rotation vector is parallel to the velocity vector. In that case, however, $(\nabla \times \mathbf{v}) \times \mathbf{v}$ vanishes. Then the nonlinear terms $(\nabla \times \mathbf{v}) \times v$ and $\nabla \times [(\nabla \times \mathbf{v}) \times \mathbf{v}]$ in the momentum budget Equation (6) and in the rotation budget Equation (7) drop out. As the nonlinear terms are responsible for the energy cascade from large to small scales the dissipation is reduced in helical flows and the lifetime of helical flow structures is increased.

LILLY (1984) showed that the rotation of thunderstorm supercells is a main reason for their stability and durability and hence for their predictability. If we apply these arguments to the rotating clouds we find that they should have longer lifetimes compared with nonrotating ones under identical forcing conditions.

This, however, has to be confirmed by observations.

It should also be kept in mind that lifetime to a large degree is dependent upon the steadiness of forcing.

The durability of rotating clouds and of the vortices in which they are embedded may in turn contribute to the observed long persistence of cloud streets. LEVICH and TZVETKOV (1984) pointed out the roll of helicity in what they called inverse energy cascade. Energy is there transported from small scales to larger scales. In our case the rotating clouds on the cloud scale would feed energy to the larger scale roll circulation thus constituting a feed back mechanism between both scales.

Helicity can only be an important controlling factor of flow development, if it is maintained over long enough times. The maintenance of helicity can be illustrated by the budget equation for helicity H, which can be derived from the vorticity equation (2):

$$\frac{D}{Dt}\rho H = -\rho \mathbf{v}\cdot\{(\nabla\mathbf{v}\cdot\nabla)\times\mathbf{v}\} - \{(\nabla\times\mathbf{v}) - \frac{1}{\rho}(\mathbf{v}\times\nabla\rho)\}\cdot\nabla p - \rho\zeta g \tag{8}$$

The shear term of the rotation budget (cf. Equation 2) leads to a helicity production term $-\rho\mathbf{v}\cdot\{(\nabla\mathbf{v}\cdot\nabla)\times\mathbf{v}\}$.

This term can also be written as:

$$\rho\mathbf{v}\cdot\{(\nabla\times\mathbf{v})\cdot\nabla\mathbf{v}\} - \rho H\nabla\cdot\mathbf{v}$$

From the first term a production term:

$$\rho\zeta w(\partial_x u + \partial_y v)$$

can be separated, which corresponds to the divergence term in the vorticity budget. It shows that helicity is produced (with positive or negative sign) if the product of vorticity, vertical velocity and horizontal divergence is unequal zero. This condition is fulfilled in the central core of the roll circulation system.

Equation (8) also shows that buoyancy combined with vorticity produces helicity. This means that the vortices in the central core are favored by buoyancy. If buoyancy is raised by release of latent heat helicity is enhanced, and the resulting vortex cloud is stabilized as a dynamical structure. Buoyancy itself is augmented by advection of water vapor to the central updraft core ("cloud source region").
As a result helicity is produced on a time scale comparable to the lifetime of the vortices.

It should be noted that helicity can only develop if the flow is three dimensional (LEVICH and TZVETKOV, 1984) with nearly identical length scales $L_x \sim L_y \sim L_z$. For single not merged clouds we have $L_x \sim L_y$ and as the height of the cloud is approximately twice its width, the relations $L_z \sim L_x$ and $L_z \sim L_y$ are also fulfilled. If the flow is two dimensional and e.g. bands of clouds or fog form as shown by the investigations of WALTER and OVERLAND (1984), then obviously no cloud rotation can occur. The same holds for merging clouds. It is reasonable to assume that even then vortices are found in the central updraft core produced by the illustrated mechanisms. They, however, are not congruent with the clouds and should be smaller in scale. Possibly they contribute to the observed modulations of the clouds along the street axis. Cloud rotation, as a consequence, can only be expected if single clouds with $L_x \sim L_y \sim L_z$ exist.

These arguments show that some interesting features of rotating clouds are found if their helicity is studied. Our knowledge of helicity in atmospheric flows, however, is still very poor and consequently the helicity considerations might be speculative. Therefore, it has to be stressed that the main conclusions of this paper do not base on the helicity arguments. Helicity is seen as an interesting quantity and a quite sensitive indicator for scale interaction processes.

As a result of these theoretical considerations we identified advection and vorticity production as two important processes with which the roll circulation influences the cloud scale motion. Cloud rotation can be explained by these two processes.

3 Observations

Central part in the physical picture just developed is the vertical rotation of clouds within cloud streets.

To the author's knowledge no observations of clouds have been reported so far, which show that clouds within cloud streets rotate.

LM1, LM2, and LMP investigated thoroughly the roll street circulation but have performed neither a vorticity analysis nor an investigation of cloud rotation. The spectral analysis which they made indicated a peak at cloud street wavelength for the horizontal wind components. This peak was also found in heights well below cloud base, similar to the results of BRÜMMER et al. (1982). However, no systematic correlation between the wind components was found. If the spectral peak is caused by vortices, then a systematic correlation between horizontal wind components should be found. The discrepancy between theory and previous observations may be a sampling effect, because a vortex is not met at each traverse of a roll by an aircraft. The same holds for ground-based measurements. Statistics are poor and the rotation may still be hidden.

In addition rotation is not easy to detect by common time series analysis because altogether four scales are involved: the mean wind, the roll circulation, the cloud scale motion, and the turbulent motions.

The results of LM1, LM2, and LMP, therefore, neither support nor contradict the developed picture.

Data for this study were collected with the Falcon aircraft during the KonTur experiment in 1981. The Falcon aircraft of the DFVLR Oberpfaffenhofen is a two engine jet which is equipped for turbulence and cloud microphysical measurements (HAUF, 1984). The three wind components are measured with a five-hole-pressure probe and corrected with the aircraft velocity determined by an inertial navigation system. Absolute errors in wind speeds are about 0.5 m/s but errors for the fluctuating wind components, which are used in the analysis, are about 0.1 0.2 m/s. The sampling rate of data is 100 Hz for the turbulent quantities and 10 Hz for lower frequency data like aircraft data.

Intercomparison flights (NICHOLLS et al., 1983) demonstrate the capability of the aircraft and its instrumentation.

Cloud microphysics data were measured with a Knollenberg-FSSP-probe.

The KonTur experiment was performed in late summer 1981 over the North Sea in the German Bight (HOEBER, 1982). Its main objective was the study of convective structures like rolls, open and closed cells.

During four days of the observation period cloud streets were investigated. In this paper results are presented from the 20th of September 1981. Details are reported by BRÜMMER et al. (1982) and by BRÜMMER (1985). The orientation of the cloud streets was nearly parallel to the layer averaged wind. The depth of the convective layer was 1200 m including a 400 m deep cloud layer based at about 850 m.

The average cloud street spacing was about 3.7 km. Wind at 160 m was blowing from 220–230° at a speed of about 17 m/s. The air temperature near the surface was about 16 °C and the sea surface temperature varied between 14.5 and 16.0 °C.

Falcon flights were performed in four heights 100 m, 660 m, 830 m and 930 m. The flight pattern was L-shaped with one leg perpendicular to the cloud streets. The flight speed was about 100 m/s.

In the following case study data from flight tracks perpendicular to the cloud streets at a height of 930 m are analyzed.

4 Results

4.1 Time series analysis

The time series of various quantities are shown in Figure 4. Data were recorded on a flight perpendicular to the cloud streets at a height of 930 m. Data are averaged over one second which is equivalent to 100 m flight path. Cloud street passages can be recognized from the radiation signal. Note that crossing a cloud street does not necessarily mean that a cloud is traversed.

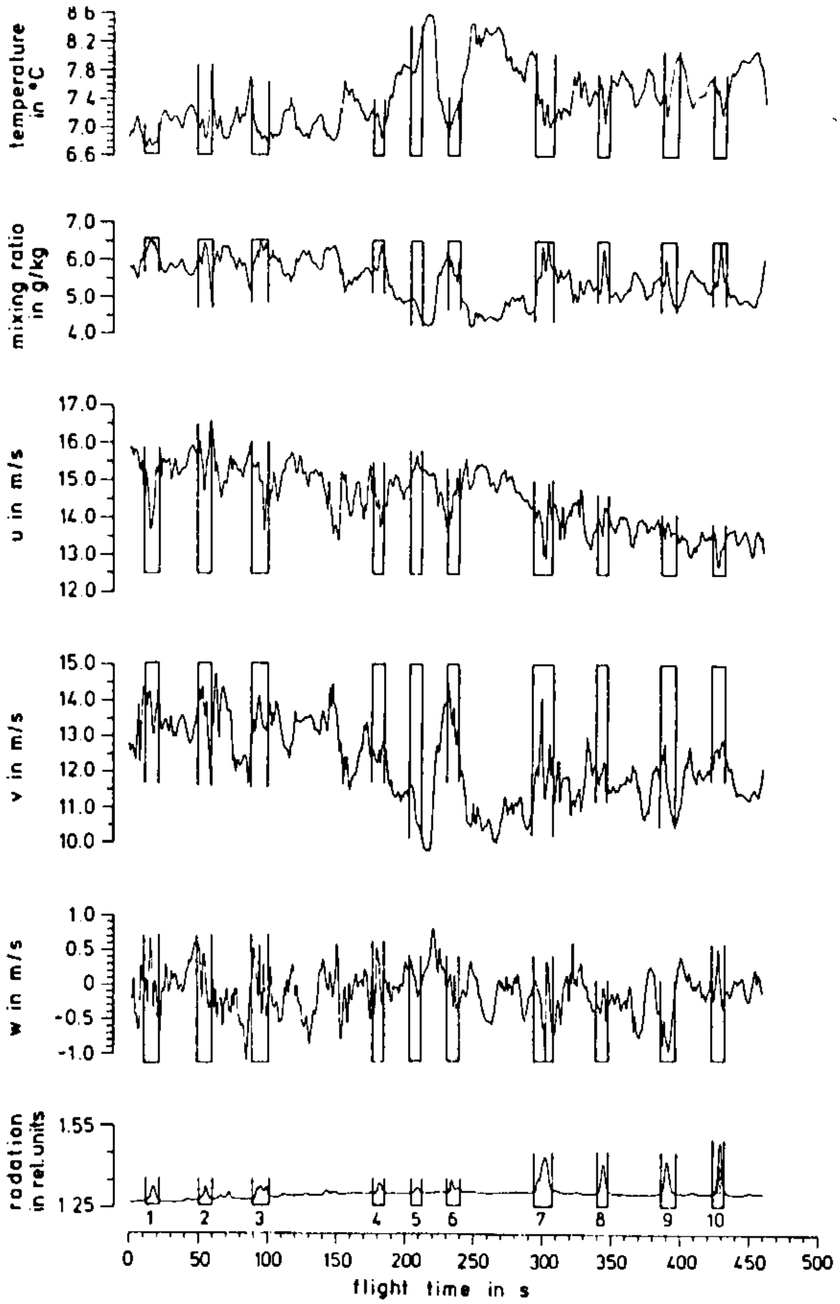

• **Figure 4**
Time series of the three wind components in a geographic coordinate system, temperature, mixing ratio and long wave downward radiation. One second flight time is equivalent to 100 m flight path. All quantities are averaged over one second. Lines indicate clouds as determined from the radiation signal.

Cloud traverses lead to peaks in the mixing ratio, but no systematic influence is found in the temperature trace. This indicates low buoyancy of the cloud in agreement with LMP's findings of relatively passive clouds in roll circulation systems. The vertical wind component shows maxima for all cloud passages. However, there also exist maxima outside of clouds, indicating turbulent eddies on the kilometer scale. The horizontal wind components show systematic variations at each cloud passage with strong extremes in contrast to LMP's observations. Also a trend can be seen in the wind data. Spacing of cloud streets varies between 2.7 km and 6 km. The same cloud street system is described and investigated by BRÜMMER (1985) and we refer to him for further information.

4.2 Spectral analysis

Spectral analysis was performed by BRÜMMER et al. (1982) and by BRÜMMER (1985). They analyzed flight legs perpendicular to the cloud streets at four heights. Results are shown in in Figure 3. The variance spectra of temperature, mixing ratio and the three wind components show pronounced maxima at wavelengths between 2–5 km (equivalent to 2 5×10^{-2} Hz for 100 m/s flight speed), which are due to the cloud street circulation. Flights in the lowest height of 100 m demonstrate that in this height turbulent fluctuations are dominant. From the time series analysis we know that with each cloud traverse strong fluctuations of the horizontal wind components are correlated. It is obvious that these fluctuations contribute a major part to the observed spectral energy at cloud street wavelength. Thus not only the roll circulation itself but also the flow structures associated with it determine the spectral energy at cloud street wavelength.

Figure 3 shows that spectral peaks in u and v at cloud street wavelength are also present in the lowest height of 100 m. If these peaks are associated with the roll circulation it shows the extension of the circulation down to near the ground. This is confirmed by an analysis of the roll circulation wind field done by BRÜMMER (1985) (cf. Figures 7a, b and Figures 2a, b, c ibid.). The peaks, however, could also indicate the vortices captured in the central updraft core. In that case vortex stretching by the central updraft possibly extends the vortices to heights below the roll circulation. No final answer can be given because a detailed analysis of the flight in 100 m was not performed.

4.3 A simple vortex model

In the following the horizontal wind field is investigated, which can be expected if a vertical rotating cloud is traversed by an aircraft. Similar to a Rankine vortex a horizontal wind field is defined (Figure 5):

$$\mathbf{v} = \Omega R \sin(r/R\,\pi)\,\mathbf{e}_\varphi + U_r \mathbf{e}_r \qquad |r| < R \tag{9}$$

with R vortex radius, Ω the maximum angular velocity, U_r the radial outflow velocity, and $\mathbf{e}_\varphi$, $\mathbf{e}_r$ unit vectors. A positive and constant outflow velocity is assumed for reasons of simplicity.

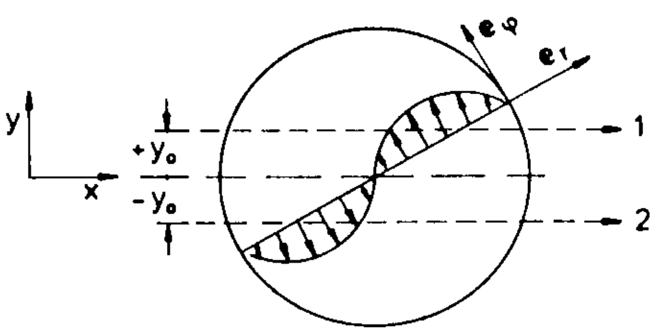

Figure 5
Sketch of a hypothetical vortex with radial distribution of horizontal wind vectors; $r^2 = x^2 + y^2$, y_0 is the distance between flight path and vortex centre.

Thus the windfield is divergent with $\nabla \cdot v = U_r/r$ and with a vorticity value of $\zeta = \Omega\pi\cos(\frac{r}{R}\pi) + \Omega(\frac{R}{r})\sin(\frac{r}{R}\pi)$.

To specify the expected wind field along a vortex traverse, three characteristic quantities have to be distinguished:

1. Direction of rotation:

   $\Omega < 0$ clockwise rotation (index a),
   $\Omega > 0$ counter-clockwise rotation (index z)

2. Radial flow U_r:

   outflow $U_r > 0$,
   inflow $U_r < 0$

3. Position of the vortex centre in relation to the flight path:

   vortex centre to the left (index 2)
   or
   right of the flight path (index 1)

Assuming a positive radial outflow, two other quantities have to be specified. Using a Cartesian coordinate system with the x-axis in flight direction four different characteristic wind distributions along the flight path are found with Equation (9) as illustrated in (Figure 6). Thus the direction of rotation and the position of the vortex centre can be derived from a measured horizontal wind field if the wind field is presented in a coordinate system aligned with the flight path. Wind blowing first from the left to the right and in the second half of the traverse from the right to the left indicates counter-clockwise rotation. In the middle of the vortex traverse the wind is blowing either parallel or antiparallel to the aircraft motion. According to this the position of the vortex centre in relation to the flight path is determined.

The vortex defined by Equation (9) is a simplification of a real vortex. However, it illustrates the basic features. It serves as a guide for identifying vortices and their main characteristics from measured wind-fields.

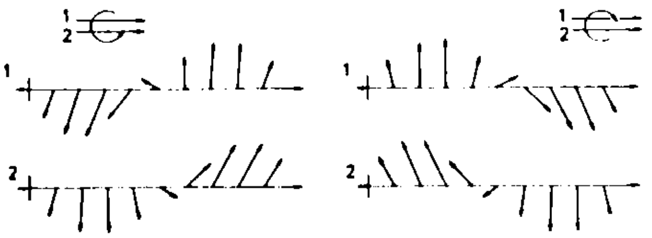

Figure 6
Horizontal wind vector for four vortex traverses with vortex centre right (1) or left (2) of flight path, and clockwise (right figures) or counter-clockwise (left figures) sense of rotation.

4.4 The wind field

Using the guide line developed in the last section, the wind field along the flight path is analyzed, see Figure (7). Mean and linear trend have been removed from the data. Wind components were transformed in a flight coordinate system. Cloud boundaries are determined either by radiation or cloud droplet concentration measurements.

Figure 7 shows the main observational result. With each cloud traverse a wavy structure in the wind vector field is correlated which is typical for a vortex.

These vortex structures, however, are also found outside of clouds. Therefore, the spectral analysis does not show a single peak for the power spectra of the horizontal wind components at the cloud street wavelength but a broader spectral band.

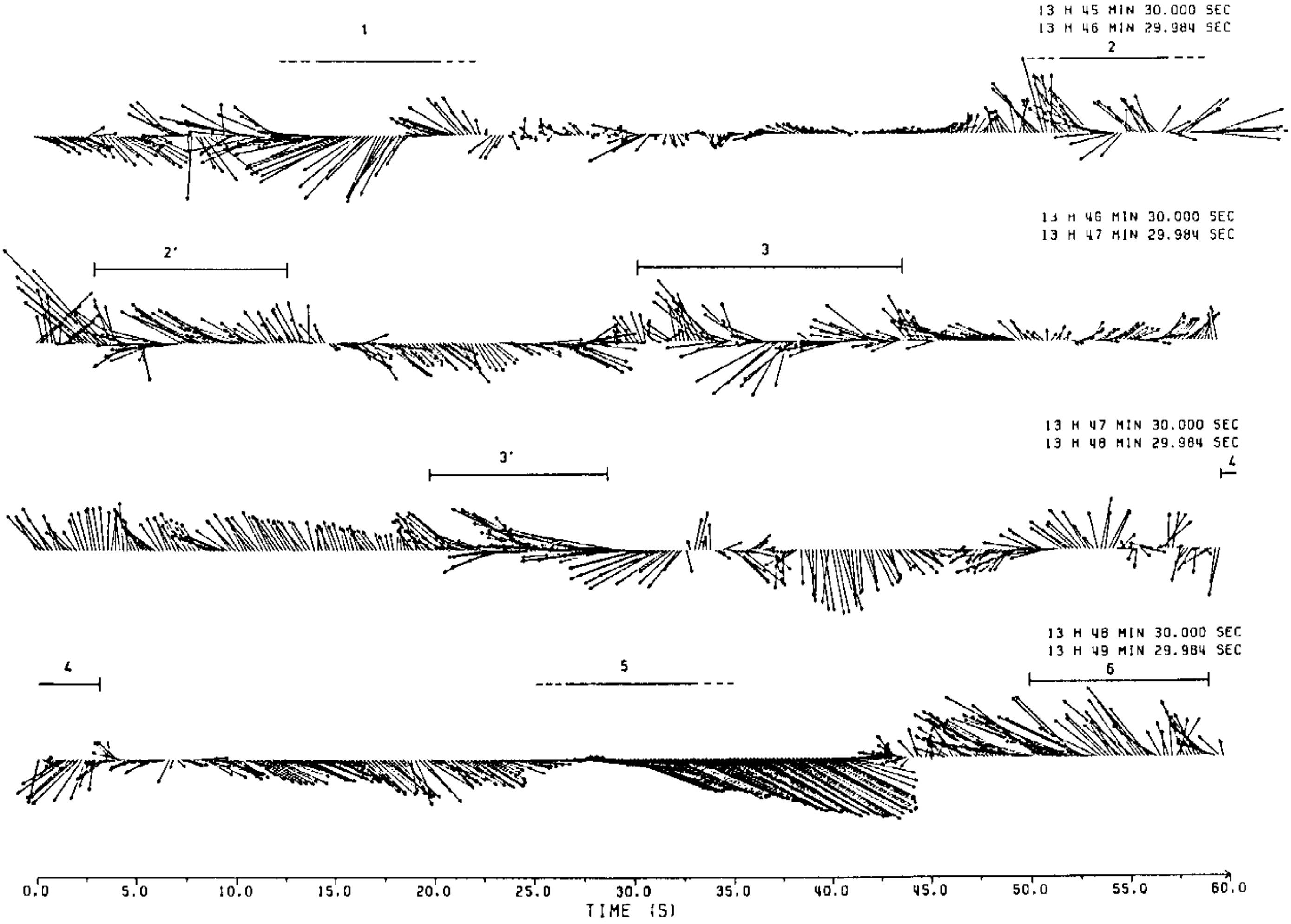
13 H 45 MIN 30.000 SEC
13 H 46 MIN 29.984 SEC
1
2
13 H 46 MIN 30.000 SEC
13 H 47 MIN 29.984 SEC
2'
3
13 H 47 MIN 30.000 SEC
13 H 48 MIN 29.984 SEC
3'
4
13 H 48 MIN 30.000 SEC
13 H 49 MIN 29.984 SEC
4
5
6
0.0
5.0
10.0
15.0
20.0
25.0
30.0
35.0
40.0
45.0
50.0
55.0
60.0
TIME (S)

a)

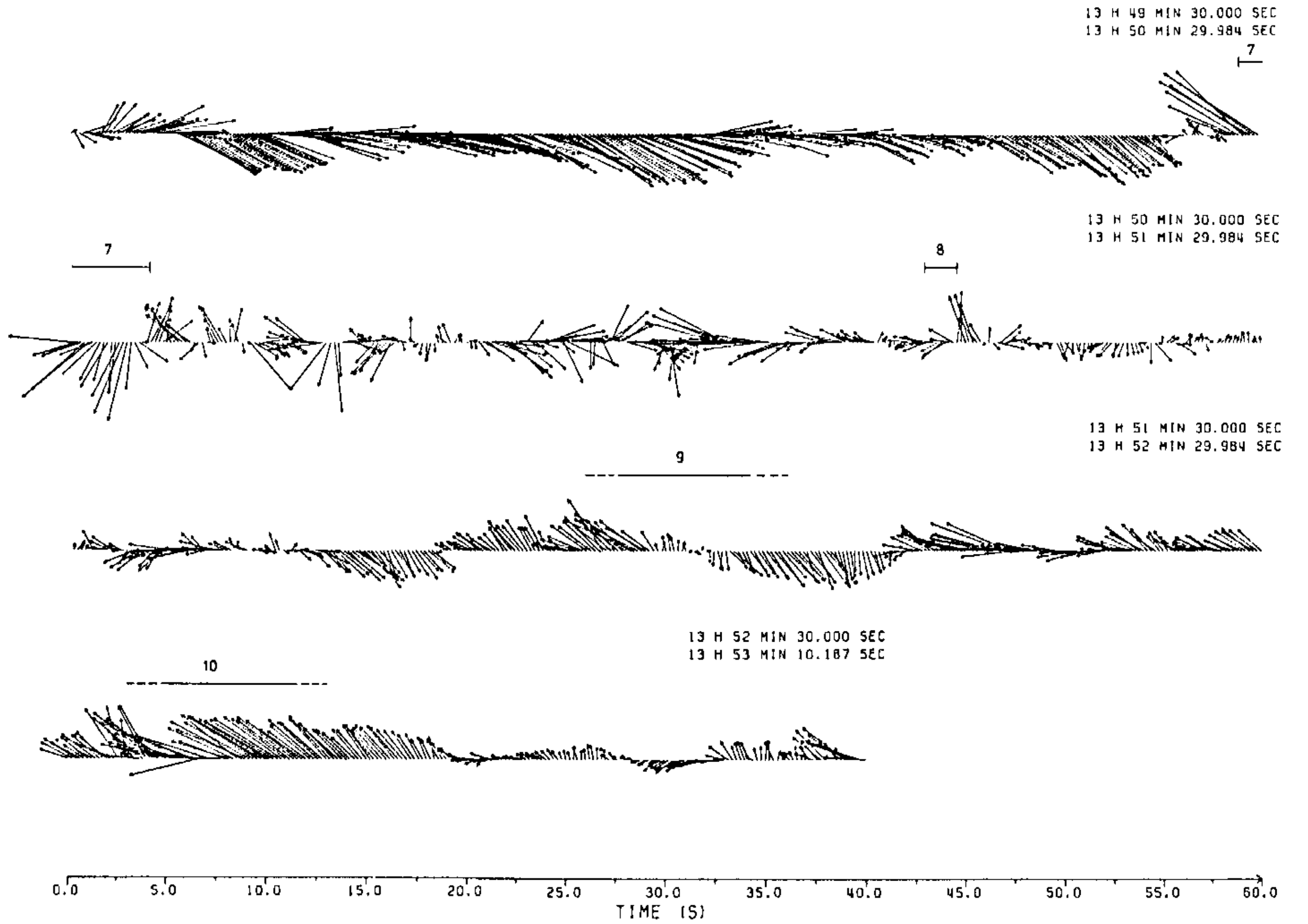
13 H 49 MIN 30.000 SEC
13 H 50 MIN 29.984 SEC
7
13 H 50 MIN 30.000 SEC
13 H 51 MIN 29.984 SEC
7
8
13 H 51 MIN 30.000 SEC
13 H 52 MIN 29.984 SEC
9
13 H 52 MIN 30.000 SEC
13 H 53 MIN 10.187 SEC
10
0.0
5.0
10.0
15.0
20.0
25.0
30.0
35.0
40.0
45.0
50.0
55.0
60.0
TIME (S)

b)

Table 1 Characteristic features of twelve investigated clouds. Cloud diameter determined by microphysics measurements (not available for clouds 1, 2, 5, 9, 10).

No	diameter of cloud	sense of rotation	position of center	U_φ	pattern	vortex diameter
1	not determined	counterc.	left	1.7 m/s	ideal	900 m
2	not determined	clockwise	left	1.7 m/s	modified	500 m
2'	980 m	counterc.	right	1.7 m/s	modified	1200 m
3	1200 m	clockwise	left/middle	1.7 m/s	strong	700 m
3'	890 m	clockwise	left	1.8 m/s	ideal	1100 m
4	330 m			1.7 m/s	not identified	not determined
5	below cloud	clockwise	right	1.5 m/s	large	1800 m
6	913 m			1.9 m/s	not identified	not determined
7	147 m	clockwise	left	2.7 m/s	strong	560 m
8	167 m	counterc.	right	1.5 m/s	modified	480 m
9	not determined	clockwise	right	2.0 m/s	large	2300 m
10	not determined	clockwise	middle	1.4 m/s	modified	680 m

Twelve clouds were traversed and the characteristic features are summarized in Table 1. In two cases the vortex pattern could not be identified but it is clearly recognizable in all other traverses. The sense of rotation or the sign of vorticity is three times more frequent clockwise than counter-clockwise. Statistics, however, is too poor for final conclusions concerning a predominant sense of rotation.

The position of the vortex centre relative to the flight path is nearly equally distributed as expected.

The maximum rotation velocity is about 1.8 m/s on the average, one-tenth of the mean wind speed. Therefore, the rotation is not very remarkable in a time series plot of the absolute wind components. Only with the aid of vector plots of the fluctuating part the rotation patterns can be identified.

The patterns themselves vary in size and structure indicating the turbulent character of the boundary layer flow. The vortex diameter varies between 500 m and 2300 m and is comparable to cloud diameter. On the average vortex diameter is a little bit greater than cloud diameter. It should be noted, however, that cloud diameters derived from droplet concentration measurements are smaller than the apparent visible diameter, because usually patches of cloudy air within a cloud are traversed only and holes of cloud-free air are found. The scatter in cloud diameter is also an effect of likelihood to meet a cloud on a straight flight path. Obviously the length of a cloud traverse depends on the distance from the cloud centre.

Questions arise whether the observed signature in the vector plot can be attributed to a vortex embedded in the roll circulation or to the roll circulation itself. If only the pure roll motion is investigated one could expect a similar signature to the one observed. This signature is caused by upward transport of low momentum and, vice versa, downward transport of high momentum. The length scale there is identical to the cloud street spacing. The observed average vortex diameter, however, is about 765 m excluding the two large vortices 5 and 9 and hence by a factor 5 smaller than the cloud street spacing.

• **Figure 7** Time series of fluctuating horizontal wind vector along a flight in 930 m height perpendicular to cloud streets. Spatial resolution of wind measurements is 1 m, equivalent to 100 Hz sampling rate. Wind vectors are averaged over 0.2 seconds. Lines indicate cloud edges as measured with cloud droplet spectrometer or as estimated from radiation signal (No. 1, 2, 5, 9, 10).

From this argument it seems obvious that the observed signature is caused by vortices and thus by a secondary effect. This conclusion is confirmed if we look at the wind vectors in Figure 6. We see that the increment in orientation angles changes its sign along the flight path. The horizontal wind vector of the roll circulation, however, plotted along the flight path always turns into the same direction. This is due to the constant phase shift between u and v in one level. The signature of the vector plot should also be repetative.

One can debate whether the two exceptional large vortices 5 and 9 belong to the roll circulation or not. The vortices 1 and 7 with a nearly ideal vortex pattern show quite clearly that they represent vortices and not the structure of the roll circulation itself.

Rotation could not be identified for all of the traversed clouds. This may be due to two different effects. First one has to think that not all but only a certain portion of all clouds rotate. Cloud rotation, therefore, might develop only under conditions which had not been fulfilled in each of the investigated clouds. A high level of turbulence can be one of such controlling factors.

Turbulence can also be the reason that cloud rotation was not detected for each traversed cloud. This means that the cloud still rotates but that the signature in the wind vector field along the flight path, which was used as criterium for cloud rotation, was covered by turbulent fluctuations so that it could not be identified. A repeated traverse of the same cloud, which, however, is very difficult to perform, would possibly show the cloud rotation.

The answer to these questions can be given only by an analysis of a greater number of cloud traverses.

Questions arise concerning the direction of rotation. The preference of clockwise rotation needs confirmation with more statistical confidence. If such a preference is found it would be interesting to look for possible mechanisms.

No attempt was made to separate motions on the roll and on the cloud scale. The spectral analysis does not show any notable spectral gap between the roll scale, the cloud scale, and the turbulence scale. Therefore, filtering of time series to separate scales would require a priori assumptions. Quantitative results would strongly depend on these assumptions and therefore would be not very reliable.

Using a special averaging technique BRÜMMER (1985), however, could resolve the roll scale motion qualitatively.

Except removing linear trend and mean value no other filtering of data was performed in this study. The main objective of this paper is to give experimental evidence of cloud rotation and this effect can clearly be seen in the data without using complicated data processing techniques like the ones developed by LM1.

4.5 Traverse of a single cloud

One of the ten cloud traverses (No. 7 in Figure 7) is investigated in more detail, mainly to illustrate the three-dimensional structure of the cloud. For this reason the following quantities are plotted in Figure 8 for 14 seconds equivalent to 1.4 km flight path:

(i) the vertical wind velocity w in m/s;

(ii) the horizontal wind fluctuation vector $\mathbf{v}_h'$, where the u-component is parallel and the v-component perpendicular to the flight direction, i.e. perpendicular and parallel to the cloud street orientation. The average wind speed over the total flight path is 18.4 m/s and the wind direction 210°;

(iii) the vertical wind variance w'^2;

(iv) the turbulent kinetic energy $(u'^2 + v'^2 + w'^2)/2$.

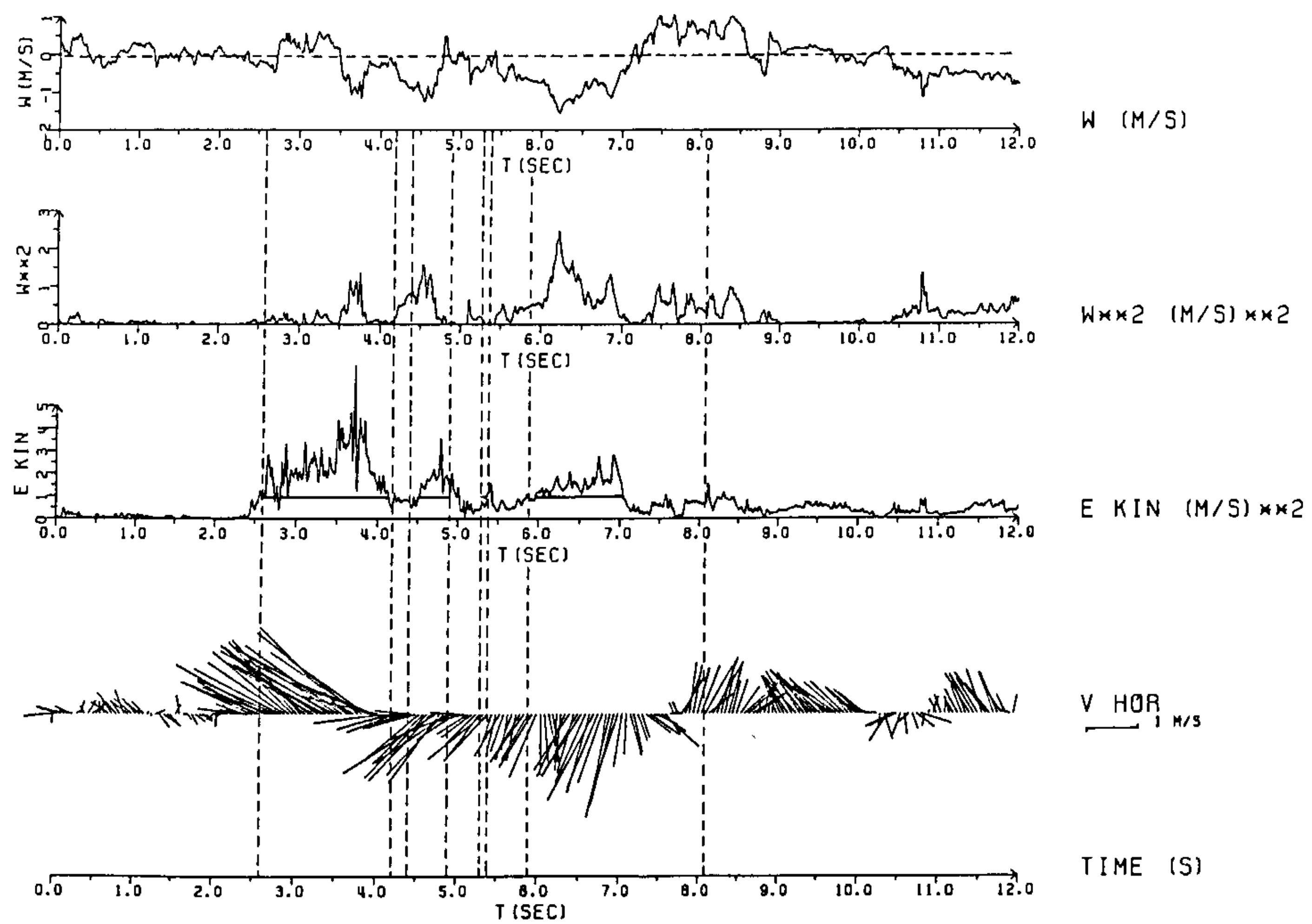

• **Figure 8** Highly resolved time series of the vertical wind component w along the flight path perpendicular to the cloud streets and of horizontal wind vectors v_h', vertical wind variance w'^2 and turbulent kinetic energy $(u'^2 + v'^2 + w'^2)/2$. Dotted lines indicate cloud boundaries. The traversed cloud is sketched in the middle of Figure 2. Wind vectors v_h' represent the deviation of the measured wind vector to the mean wind vector averaged over 5 m, all other quantities are plotted for each 0.01 s = 1 m.

Data is plotted for each 0.01 s (≡ 1 m). Horizontal wind vectors, however, are averaged over 0.05 s (≡ 5 m). Cloud edges are indicated by dotted vertical lines.

The cloud itself consists of two main bodies with some cloud patches in between. The diameter of the main parts is about 180 m and their horizontal separation is 200 m, so that the cloud traverse has a total length of 560 m. Looking at the vertical wind field a similar pattern and symmetric structures are found with rising air motions at the cloud edges and subsidence in the central part. The average of the vertical wind speed along the cloud traverse is negative, so that it is assumed that the cloud is in its late stage. This hypothesis is confirmed by the cloud average temperature deviation which is also negative. The strongest negative temperature deviation is found in the inner sinking part indicating a cold downdraft.

The findings agree well with the passive character of roll circulation clouds found by LMP. These clouds, in contrast to purely convective buoyant clouds, are more or less forced by the larger scale roll circulation. Buoyancy, therefore, is less than in convective clouds.

The most striking feature of the cloud is its horizontal air motion. Changes of wind direction of the fluctuating part up to 180° are found from one cloud edge to the other. Figure 8 shows a nearly sinusoidal wave confined to the cloud region. The symmetry is not as perfectly expressed as for the vertical wind. The figure immediately suggests the hypothesis of a rotating ring cloud with rising motions at the edges and sinking motions in its centre. The principal structure of the cloud is sketched in Figure 2.

Another noteworthy result is the strong correlation of turbulent kinetic energy and cloud presence. Vertical wind as well as its variance are less correlated.

A threshold value for turbulent kinetic energy, arbitrarily defined at 1 m^2/s^2 gives exactly the clouds and cloud patches.

This indicates the strong coupling of cloud microphysics and turbulence, which, however, is not subject of this paper.

5 Summary

In a case study a maritime cloud street system was investigated. Aircraft measurements show that most of the clouds were found to be embedded in a vortex with vertical axis of rotation. The vortex diameter was about 500 m – 2300 m and comparable to the cloud diameter. Maximum rotation velocity was about 2 m/s. No preferred sign of rotation was found. The rotation is explained with the aid of the vorticity equation by considering the advection process and the vorticity production caused by the convergence in the lower half of the roll circulation system. Both processes represent scale interaction mechanisms between the roll scale and smaller scales as the cloud scale and the turbulent scale. Consequently two different cases were considered:

(i) impact of roll scale motion on turbulent motion.

By advection moisture, turbulent kinetic energy and vorticity are transported to the central updraft core. Also small scale flow structures within the circulation system like thermals or eddies are collected there. The strong convergence of the wind field acts as a source for vorticity production. Preexisting vorticity associated with the thermals is amplified and finally they rotate. They merge and increase in size up to some characteristic length scale which is determined by a process not investigated in this paper.

The central updraft stretches the vortices. Their vorticity is continuously enhanced till some equilibrium value is reached. Altogether the vortices are captured in the central updraft core. They possibly extent over the whole convective layer. The updraft is concentrated in the vortices. Clouds, therefore, are embedded in vortices and rotate.

(ii) impact of roll scale motion on cloud scale motion.

The cloud scale with individual clouds is assumed to be given. Advection arranges the clouds and likewise any other convective elements of similar size in lines along the updraft core. It also supplies the clouds with moisture, heat, turbulent kinetic energy and vorticity. Preexisting vorticity associated with the clouds is continuously amplified so that the clouds finally rotate.

The two cases differ in to what extent advection and vorticity production determine the scaling mechanism of clouds. No final answer can be given by the observational material presented in this paper. It will be the objective of future numerical investigations to clarify the problem of cloud scaling. Rotation of clouds may possibly play a decisive role there. One major consequence of cloud rotation concerns the helicity $H = \mathbf{v} \cdot (\nabla \times \mathbf{v})$ which for rotating clouds is higher than for nonrotating ones. The helicity concept offers some interesting aspects of cloud rotation. Rotating clouds should have a higher lifetime compared to nonrotating clouds. Cloud rotation can only occur if all three length scales of the cloud are nearly identical. The rotation of clouds can contribute to the long persistence of cloud streets

thus indicating a feed back mechanism between the cloud scale and the roll scale. It also represents an energy transfer from small scales to larger scales as part of an inverse energy cascade which is typical for helical flows.

These findings, however, should be confirmed by more observations.

6 Acknowledgements

Part of this work was supported by the Deutsche Forschungsgemeinschaft, whose help I gratefully want to acknowledge. I also want to thank Prof. HINZPETER for enabling the participation in the KonTur experiment and for providing the data. I appreciate the help of many colleagues at the Meteorologisches Institut Universität Karlsruhe and at the Institut für Physik der Atmosphäre, DFVLR Oberpfaffenhofen. Thanks are also given to B. BRÜMMER, H. SCHLÜNZEN and W. BÖGEL for data processing and for the spectral analysis.

List of Symbols

x, y, z	Cartesian coordinates
$\mathbf{i}, \mathbf{j}, \mathbf{k}$	Cartesian unit vectors
$\mathbf{e}_\varphi, \mathbf{e}_r$	unit vectors in cylindrical coordinates
$\partial_t, \partial_x, \partial_y, \partial_z$	partial derivatives
$\partial/\partial t, \partial/\partial x, \partial/\partial y, \partial/\partial z$	partial derivatives
∇	gradient operator
∇_h	horizontal gradient operator
$D/Dt\, \rho\phi = \partial\rho\phi/\partial t + \nabla \cdot \mathbf{v}\rho\phi$	budget operator
$\mathbf{v}$	wind velocity vector
$\mathbf{v}_h$	horizontal wind vector
u, v, w	Cartesian wind components
ρ	density
p	pressure
g	gravity
Ω	angular velocity
U_r	radial velocity
U_φ	rotation velocity
$\nabla \times \mathbf{v}$	rotation or vorticity
$\zeta = \mathbf{k} \cdot (\nabla \times \mathbf{v})$	vertical component of vorticity
$H = \mathbf{v} \cdot (\nabla \times \mathbf{v})$	helicity
R	radius

References

BROWN, R. A., 1980: Longitudinal instabilities and secondary flows in the planetary boundary layer: a review. Review of Geophysics and Space Physics 18, 683–697.

BROWN, R. A., 1974: Analytical methods in planetary boundary-layer modelling. Adam Hilger, London.

BRÜMMER, B., SCHLÜNZEN, H. and BÖGEL, W., 1982: Cloud streets during KonTur. In: KonTur.Convection and turbulence experiment. Preliminary results. Hamburger Geophysikalische Einzelschriften, Reihe A, Heft 57, 63–77.

BRÜMMER, B., 1985: Structure, dynamics and energetics of boundary layer rolls from KonTur aircraft observations. Beitr. Phys. Atmosph. 58, 237–254.

ETLING, D., 1985: Some aspects of helicity in atmospheric flows. Beitr. Phys. Atmosph. 58, 88–100.

HAUF, T., 1984: Turbulenzmessungen mit dem Forschungsflugzeug Falcon. Meteorol. Rdsch. 37, 163–176.

HOEBER, H. C., 1982: KonTur. Convection and turbulence experiment. Field phase report. Hamburger Geophysikalische Einzelschriften, Reihe B, Heft 1.

KUETTNER, J., 1959: The band structure of the atmosphere. Tellus 11, 267–294.

KUETTNER, J., 1971: Cloud bands in the earth's atmosphere. Tellus 23, 404–426.

LeMONE, M. A., 1973: The structure and dynamics of horizontal roll vortices in the planetary boundary layer. J. Atmos. Sci. 30, 1077–1091.

LeMONE, M. A., 1976: Modulation of turbulence energy by longitudinal roles in an unstable planetary boundary layer. J. Atmos. Sci. 33, 1308–1320.

LeMONE, M. A. and PENNELL, W. T., 1976: The relationship of tradewind cumulus distribution to subcloud layer fluxes and structure. Mon.Wea. Rev. 104, 524–539.

LEVICH, E. and TZVETKOV, E., 1984: Helical inverse cascade in three-dimensional turbulence as a fundamental dominant mechanism in mesoscale atmospheric phenomena. To be published in Phys. Rep.

LILLY, D. K., 1984: Helicity as a stabilizing effect on rotating convective storms. Submitted to J. Atmos. Sci.

MÜLLER, D., 1984: Untersuchung der dynamischen Bedingungen zur Wolkenstraßenbildung über Norddeutschland mit Hilfe aerologischer Routinemessungen. Dipl.Arbeit, Inst. Met. u. Klimatologie, Universität Hannover.

NICHOLLS, S., SHAW, W. and HAUF, T., 1983: An intercomparison of aircraft turbulence measurements made during JASIN. J. Climate Appl. Met. 22, 1637–1648.

WALTER, B. A. and OVERLAND, J. E., 1984: Observations of longitudinal rolls in a near neutral atmosphere. Mon. Wea. Rev. 112, 200–208.